Ultramicroscopy 146 (2014) 125–129

Contents lists available at ScienceDirect

Ultramicroscopy

journal homepage: www.elsevier.com/locate/ultramic

In situ electron holographic study of Ionic liquid

Manabu Shirai [a,*], Toshiaki Tanigaki [a,b], Shinji Aizawa [b], Hyun Soon Park [b,1], Tsuyoshi Matsuda [c], Daisuke Shindo [b,d]

[a] Hitachi, Ltd., Central Research Laboratory, Hatoyama, Saitama 350-0395, Japan
[b] Center for Emergent Matter Science (CEMS), RIKEN, Hirosawa 2-1, Wako, Saitama 351-0198, Japan
[c] Japan Science and Technology Agency, Kawaguchi, Saitama 332-0012, Japan
[d] Institute of Multidisciplinary Research for Advanced Materials, Tohoku University, Katahira 2-1-1, Sendai 980-8577, Japan

ARTICLE INFO

Article history:
Received 13 February 2014
Received in revised form
25 July 2014
Accepted 3 August 2014
Available online 10 August 2014

Keywords:
Electron holography
Ionic liquid
Electron irradiation
Electrostatic potential
Charge

ABSTRACT

Investigation of the effect of electron irradiation on ionic liquid (IL) droplets using electron holography revealed that electron irradiation changed the electrostatic potential around the IL. The potential for low electron flux irradiation (0.5×10^{17} e/m^2 s) was almost constant as a function of time (up to 180 min). For higher electron flux irradiation (2×10^{17} e/m^2 s), the potential increased exponentially for a certain time, reflecting the charging effect and then leveled off. The IL was found to be changed from liquid to solid state after a significant increase in the electrostatic potential due to electron irradiation.

1. Introduction

Ionic liquids (ILs) are molten salts composed entirely of ions that retain liquid state even at room temperatures. Since a stable IL was first reported in 1992 [1], many kinds of ILs have been synthesized and studied intensively because of their attractive properties, such as negligible vapour pressure, high ionic conductivity, non-combustibility, and high thermal stability [2,3]. ILs have thus attracted much research attention as new functional materials for industrial applications. For example, they are promising candidates as electrolytes for lithium-ion rechargeable batteries [4], double-layered capacitors [5], electronic devices [6], and solar cells [7]. They have been widely utilized for scanning electron microscope (SEM) observation of biological samples such as seaweed and human culture cells, because they do not vaporize even under vacuum conditions [8–10]. In addition, they behave like electrical conducting materials, so that they can provide electric conductivity to insulating materials for SEM observation. In addition, they can be used as solvents and supporting films of nanoparticles for transmission electron microscope (TEM) observation [11,12]. Furthermore, metal nanoparticles are very stable in ILs and can be observed at high resolution.

However, whether ILs remain in liquid form and whether they become charged during high-resolution TEM observations are open questions. If they become charged due to the electron irradiation and their good conductivity drops, ILs cannot be utilized for electron microscope observations. Therefore, as a first step to clarify these points, in this paper we have concentrated our attention on the study of the conductivity of ILs. For that purpose, we used electron holography [13] to analyze the electrostatic potential distributions around ILs as a function of electron beam flux and their irradiation time. Furthermore, we have investigated their surface hardness changes after the electron irradiation by using a fine tungsten probe in an SEM.

2. Experimental

We used an IL of 1-butyl-3-methylimidazolium tetrafluoroborate (BMI-BF_4) (KANTO CHEMICAL Co., Inc.). Using a focused ion beam (FIB)-SEM system (NB5000, Hitachi High-Technologies Co.), we fabricated and shaped a cuboid-shaped sample holder with 100 μm wide, 50 μm high, and 15 μm thick on Pt wire (50 μm in diameter) as illustrated in Fig. 1(a). The upper surface of the holder was smoothed to minimize the surface roughness of the Pt, to which an IL droplet was attached. The droplet size was controlled to be approximately 30 μm.

* Corresponding author. Present address: Hitachi High-Technologies Corporation, Sakado 3-2-1, Takatsu-ku, Kawasaki, Kanagawa 213-0012, Japan.
E-mail address: shirai-manabu@naka.hitachi-hitec.com (M. Shirai).
[1] Present address: Department of Materials Science & Engineering, Dong-A University, Busan 604-714, Republic of Korea.

http://dx.doi.org/10.1016/j.ultramic.2014.08.003
0304-3991/

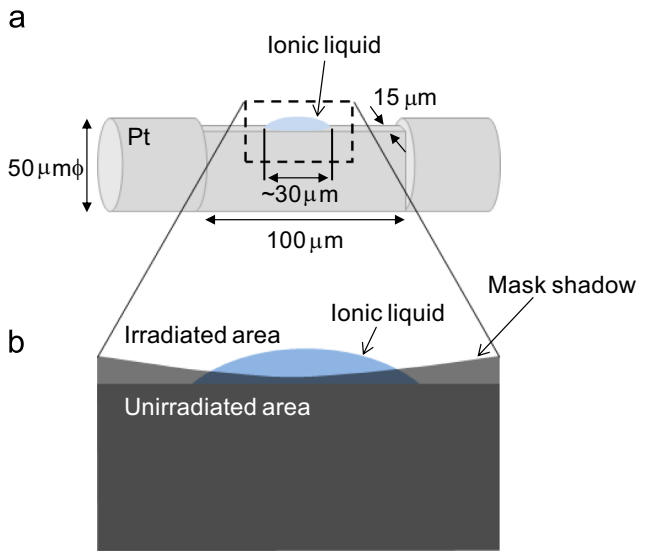

Fig. 1. Schematic illustrations of (a) ionic liquid sample position on the Pt holder and (b) experimental setting for TEM observation.

The droplet was subjected to electron irradiation during *in situ* observation inside the microscope. The electron beam flux was controlled to range from 0.5×10^{17} to 2×10^{17} e/m^2 s. Since secondary electrons emitted from the irradiated Pt wire could affect the electrostatic potential distribution (or charging) of the IL, we placed the Pt wire in the shadow of the condenser aperture used as a mask, as shown in Figs. 1(b) and 2(c), which enabled us to investigate the charging effect of only the IL induced by the electron irradiation. In an alternative experimental design without the mask shadow, both the IL and Pt wire were subjected to electron irradiation. After irradiation for 180 min, we determined the IL surface hardness by using a fine tungsten probe in the FIB-SEM. Here, solids do not change their shape while liquids change their shape in contact with the probe.

Holographic observation was performed using a TEM (HF-3300X, Hitachi High-Technologies Co.) equipped with a cold field-emission gun operated at 300 kV. Holograms were acquired using a slow-scan charge-coupled-device (CCD) camera with 4096 × 4096 pixels (UltraScan™ 4000, Gatan Inc.). Using double-biprism electron interferometry [14], we controlled the fringe spacing and interference region width independently. The fringe spacing and the field of view of the interference region were measured to be 400 nm and 30 μm, respectively. By measuring the slope of the electron phase shift at 15 μm from the droplet surface (see the vertical white line A–B in Fig. 2(a)), we evaluated the temporal change in the electrostatic potential distribution outside the IL. To investigate the electrostatic potentials of the IL surface, we performed simulation using the ELFIN/ViewField software ver. 2.0.0 (ELF Co., Japan) [15,16]. The charges were calculated using Maxwell's equations in the integral form by the ELF Integral Element Method. In the simulation, we used the experimental values measured by using an optical microscope and an SEM: the sizes of the droplet were 30 μm wide, 3 μm high, and 15 μm thick and the sizes of the substrate on which the droplet was placed at 0 V were 100 μm wide, 50 μm high, and 15 μm thick. We also set constant electrostatic potentials for all the electron irradiated areas. The modulation of the reference waves due to charging was included in the simulated phase images.

3. Results and discussion

Fig. 2(a) shows the temporal changes in the reconstructed phase images (in electron holography) for 300 kV electron irradiation with a flux of 2×10^{17} e/m^2 s. These images represent the electrostatic potential distribution outside the droplet. A hologram with the mask shadow is depicted in Fig. 2(c). The inside of the droplet could not be seen because the droplet was too thick for electrons to penetrate. The electrostatic potential distribution around the IL was observed even at the initial observation (0.13 min). The density of the contour lines in the reconstructed phase images increased with the irradiation time, which is attributed to an increase in the charging effect of the IL.

Fig. 2(b) shows the simulated phase images when the electrostatic potential of the IL surface was assumed to be 0.09 V, 0.14 V, and 0.21 V. The phase shift profiles corresponding to the A–B line are shown in Fig. 2(d). The simulation results were in good agreement with the experimental data. We converted the phase shift (rad/μm) measured at each time point into electrostatic potential (V) of the IL surface as a function of irradiation time as shown below. The small V value means that the charge effect of the IL was small.

Fig. 3(a) shows the time dependence of the IL electrostatic potential when the droplet was irradiated with an electron flux of 2×10^{17} e/m^2 s (A), 1×10^{17} e/m^2 s (B), and 0.5×10^{17} e/m^2 s (C). Because of the use of the mask shadow, only the droplet was exposed to the irradiation. The black arrows for A correspond to the reconstructed phase images in Fig. 2(a). The electrostatic potential tended to increase slightly during the first 10 min irradiation period. The changes in the potential showed different behaviors depending on the electron beam flux. The electrostatic potential for the sample irradiated with a flux of 2×10^{17} e/m^2 s (A: red circles) increased after 60 min and saturated after 130 min. For 1×10^{17} e/m^2 s (B: blue triangles), the potential increased after 120 min. In contrast, for 0.5×10^{17} e/m^2 s (C: green squares), the electrostatic potential increased slowly over time of the experiment. We note that the increase in the electrostatic potentials for A and B began at the same dose value of 7.2×10^{20} e/m^2, which we defined as the critical irradiation dose.

To directly investigate the IL surface hardness after 180 min electron irradiation, we pressed the IL surface using a fine tungsten probe and afterwards removed it from the surface in the FIB-SEM. The surface hardness profiles after irradiations of 2×10^{17} e/m^2 s (A) and 0.5×10^{17} e/m^2 s (C) are shown in the SEM images (Figs. 3(b) and (c)). Changes in the contrast of the droplet can be seen at the interface between the irradiated and unirradiated areas, as indicated by the dashed white line (trace of the mask edge) in Fig. 3(b). The difference in the IL surface hardness between these two areas is clear: the surface of the irradiated area was found to be solid since the surface was unchanged under the pressure of the probe and did not stick to the probe when it was removed. On the other hand, the surface of the unirradiated area appeared to be liquid (or gel-like), because the probe was kept clinging to IL surface when it was removed as shown in the yellow circle. The IL surface hardness of the sample irradiated with a flux of 1×10^{17} e/m^2 s for 180 min was similar to that shown in Fig. 3(b) (not shown here). In contrast, the observation results of the lowest flux irradiation (0.5×10^{17} e/m^2 s) were completely different, as shown in Fig. 3(c). The entire area of the droplet remained liquid (or gel-like) even after the electron irradiation for 180 min. It is reasonable to think that the IL should transform into a solid state after its electrostatic potential significantly increase due to electron irradiation.

Electron beam irradiation induces knock-ons and local heating of ILs. Thus, electric and mechanical properties of IL may change by electron irradiation. Onsets of the electrostatic potential increase due to electron irradiation occurred at the critical irradiation dose. This electrostatic potential dependency on dose implies IL's electron conductivity changes. The results obtained from electron holography and *in-situ* SEM observations using the probe indicated